The Route Toward a Diode-Pumped 1-W Erbium 3-μm Fiber Laser

Markus Pollnau

***Abstract*—A rate-equation analysis of the erbium 3-μm ZBLAN fiber laser is performed. The computer calculation includes the longitudinal spatial resolution of the host material. It considers ground-state bleaching, excited-state absorption (ESA), interionic processes, lifetime quenching by co-doping, and stimulated emission at 2.7 μm and 850 nm. State-of-the-art technology including double-clad diode pumping is assumed in the calculation. Pump ESA is identified as the major problem of this laser. With high Er^{3+} concentration, suitable Pr^{3+} co-doping, and low pump density, ESA is avoided and a diode-pumped erbium 3-μm ZBLAN laser is predicted which is capable of emitting a transversely single-mode output power of 1.0 W when pumped with 7-W incident power at 800 nm. The corresponding output intensity which is relevant for surgical applications will be in the range of 1.8 MW/cm^2. Compared to Ti:sapphire-pumped cascade-lasing regimes, the proposed approach represents a strong decrease of the requirements on mirror coatings, cavity alignment, and especially pump intensity. Of the possible drawbacks investigated in the simulation, only insufficient lifetime quenching is found to have a significant influence on laser performance.**

***Index Terms*— Diode-pumped lasers, infrared lasers, laser biomedical applications, optical fiber lasers, rare earth lasers.**

I. Introduction

FOR several years, there has been an increased interest in lasers emitting at 3 μm mainly because of their potential applications in laser surgery [1]. Due to the high absorption of 3-μm radiation in water, high-quality cutting or ablation is demonstrated in biological tissue using erbium-doped solid-state lasers [2], [3]. Erbium-doped fluoride fibers are promising candidates for the construction of compact and efficient all-solid-state laser sources that provide large flexibility and high laser intensity which is of relevance for surgical applications.

Recently, computer simulations of the 3-μm fiber system gave surprising answers to the main questions and strongly stimulated experimental research. First, the saturation of the output power of the erbium 3-μm ZBLAN laser was explained by excited-state absorption (ESA) and competitive lasing at 850 nm [4]. Second, the overcome of the saturation was predicted and experimentally demonstrated by upconversion-cascade lasing at 1.7 and 2.7 μm. A transversely single-mode output power of 150 mW was achieved under Ti:sapphire pumping [5]. With optimized fiber parameters, the slope efficiency could be enhanced to 25.4% [6] which represents more than 90% of the theoretical limit [7]. The requirement of high pump intensity, however, excludes the cascade regime from diode pumping. Third, the unexpectedly low performance of a different approach, the quenching of the lower laser level by Pr^{3+} co-doping [8], could be explained by insufficient quenching and the successful competition of ESA with subsequent 850-nm lasing [9]. So far, it has been possible only with ESA to overcome the bottleneck of ground-state bleaching and long excited-state lifetimes.

In this paper, a solution that allows for efficient diode pumping of the system is presented and investigated in a computer simulation. A diode-pumped erbium 3-μm ZBLAN double-clad fiber laser utilizing state-of-the-art technology is predicted which is capable of emitting a transversely single-mode output power of 1.0 W when pumped with 7-W incident power at 800 nm. The corresponding output intensity will be 1.8 MW/cm^2. Possible drawbacks of the proposed device are investigated and their influence is quantitatively analyzed.

II. The Problem of Excited-State Absorption and Its Solution

In this section, a short analysis is given of the problems that have prevented the erbium 3-μm fiber laser from delivering high output power. Although this may partly represent a review of earlier articles, it is necessary to explain the findings in a larger context in order to identify the main problem. From this analysis, the way leads directly to the solution of the problem. For the following, cf. the erbium ZBLAN level scheme given in Fig. 1.

The erbium 3-μm fiber laser could in principle be operated as a simple four-level laser. Pump absorption at 800 nm on the ground-state transition $^4I_{15/2} \rightarrow {}^4I_{9/2}$ and subsequent fast multiphonon relaxation into the $^4I_{11/2}$ upper laser level lead to inversion on the laser transition $^4I_{11/2} \rightarrow {}^4I_{13/2}$ at 3 μm. The lifetime of the lower laser level exceeds that of the upper laser level. Despite this fact, steady-state inversion can be achieved due to the favorably low branching ratio from upper to lower laser level [10].

The long lifetime of the lower laser level, however, introduces a bottleneck. The high pump intensity in a core-pumped fiber laser leads to a strong excitation rate of the system. The excited energy is stored in the long-living lower laser level and—due to threshold inversion—also in the upper laser level. This causes an almost complete ground-state bleaching and highly inefficient pump absorption. It is found experimentally that ESA from the lower laser level at 791 nm removes energy from the $^4I_{13/2}$ reservoir and indirectly—again due to the

Manuscript received April 17, 1997; revised July 31, 1997.

The author was with the Institute of Applied Physics, University of Bern, CH-3012 Bern, Switzerland. He is now with the Optoelectronics Research Centre, University of Southampton, Southampton SO17 1BJ, U.K.

Publisher Item Identifier S 0018-9197(97)07821-4.

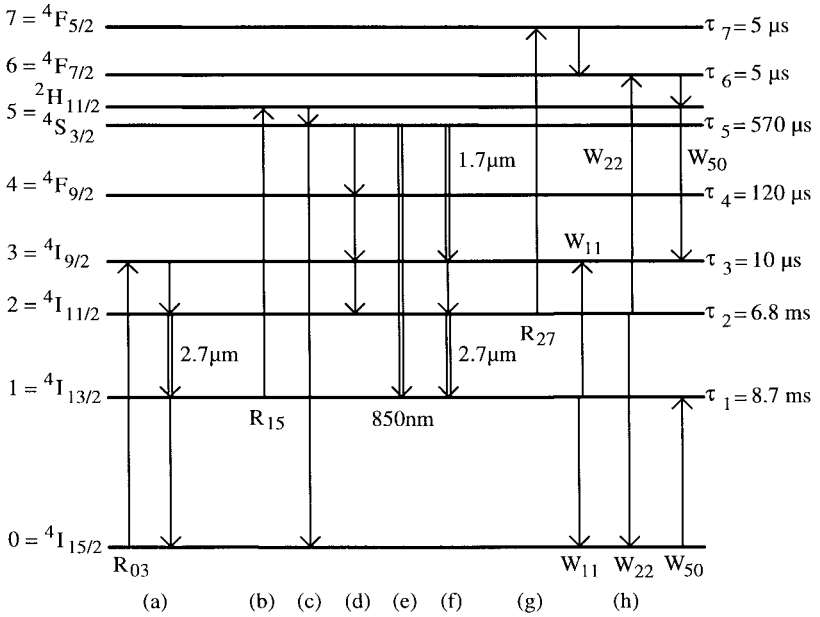

Fig. 1. Energy-level scheme of erbium in ZBLAN. R_{03}, R_{15}, and R_{27} denote the pump transitions of GSA, ESA 1 from the lower laser level, and ESA 2 from the upper laser level, respectively. 2.7 μm, 850 nm, and 1.7 μm label the laser transitions at the corresponding wavelengths. W_{11}, W_{22}, and W_{50} correspond to interionic processes. (a) Simple four-level scheme of the erbium 2.7-μm laser. (b) ESA 1 removes excitation from the $^4I_{13/2}$ reservoir which is (c) partly redistributed into the ground state via green fluorescence, (d) partly redistributed into the upper laser level via multiphonon relaxation, and partly accumulated in the $^4S_{3/2}$ level. (e) This leads to competitive lasing at 850 nm. (f) Upconversion cascade lasing at 1.7 and 2.7 μm suppresses the 850-nm line, recycles the upconverted energy, and avoids the saturation. (g) ESA 2 depletes the upper laser level. (h) Interionic processes may occur at high dopant concentration.

threshold condition—also from the $^4I_{11/2}$ upper laser level. The energy is redistributed partly into the ground state via green fluorescence. This introduces an inefficient pumping scheme, because two pump photons (GSA and ESA) are necessary for the creation of one laser photon. Another fraction of the energy is redistributed into the upper laser level via multiphonon decay. This supports lasing at 3 μm.

Thus ESA solves the bottleneck problem. Unfortunately it introduces another problem. Part of the energy is accumulated in the $^4S_{3/2}$ level which leads to lasing on the transition $^4S_{3/2} \rightarrow {}^4I_{13/2}$ at 850 nm. This second laser successfully competes with the 3-μm laser, which causes the 3-μm output power to saturate [4]. The 850-nm line can be suppressed and the energy can be guided into the upper laser level by cascade lasing on the transition $^4S_{3/2} \rightarrow {}^4I_{9/2}$ at 1.7 μm which solves the problem of uncontrolled energy redistribution from the $^4S_{3/2}$ level and avoids the saturation of the 3-μm output power [5].

Yet this causes a third problem. Inversion on the upconversion-pumped transition at 1.7 μm can only be achieved with high pump intensity. A diode-pumped high-power laser device, however, is only possible with double-clad fibers and in excitation regimes which operate at the low pump intensity that is provided by pump diodes. Thus, the highly efficient cascade-lasing system is restricted to Ti:sapphire pumping.

It is the irony of the erbium 3-μm fiber laser that the simple four-level system could well be operated at low pump intensity, if there were no ground-state bleaching. ESA from the lower laser level introduces the mentioned complications. In this paper, ESA is, for the first time, not considered as an aid to avoid ground-state bleaching, but it is identified as the major problem of this laser. Consequently, two questions arise. How can ESA be suppressed and how can ground-state bleaching be avoided without the assistance of ESA? These questions are closely related to each other.

Four possible solutions are at hand.

1) The pump wavelength can be detuned from the ESA peak. This reduces absorption on the ESA transition.
2) The dopant concentration can be increased [11]. This reduces ground-state bleaching, because a higher population is initially available in the ground state.
3) The pump wavelength can be detuned from the GSA peak. This reduces GSA and, hence, ground-state bleaching.
4) Pr^{3+} co-doping can remove energy from the lower laser level and repopulate the ground state [12], [8].

(A fifth possibility, the quenching of the lifetime of the lower laser level by interionic upconversion, is probably not of relevance; cf. Sections III and V). In recent years, all these approaches have been investigated for different reasons and independently from each other. None of them has led to a significant improvement, because these approaches do not address the two related questions simultaneously. Only lifetime quenching by co-doping depletes the ESA level and repopulates the ground state in one step. But this approach is not sufficient to prevent ESA from having a crucial influence [9].

The proper combination of the possible solutions answers both questions simultaneously and leads to the desired double-clad diode-pumped high-power device. ESA is reduced by detuning the pump wavelength from the ESA peak. An in-

creased dopant concentration favors GSA with respect to ESA [7]. In addition, it increases energy diffusion within the lower laser level and improves lifetime quenching by Pr^{3+} co-doping [12]. The quenching process weakens ground-state bleaching and population of the ESA level [9]. Detuning the pump wavelength from the GSA peak is substituted by double-clad pumping which automatically reduces GSA, ground-state bleaching, excited-state population, and ESA. The weakened pump absorption is in return compensated by higher dopant concentration. The four approaches support each other in a perfect manner.

Since double-clad ZBLAN fibers are rather expensive, it is apparent that these ideas are best investigated in computer simulations which conducted experiments so well in recent years [4], [5], [7], [9]. In addition, the understanding of the population dynamics is deepened, system parameters can be optimized, and possible pitfalls can be identified that have to be investigated spectroscopically before performing the main experiment.

III. Rate Equations

In a computer simulation considering the relevant levels (ground state and seven excited states, see Fig. 1) and processes (GSA, ESA, ground-state depletion, all lifetimes and branching ratios, lifetime quenching by co-doping, three interionic processes, stimulated emission on two multiplet transitions, and the data of fiber and resonator), time- and space-dependent rate equations describing the erbium ZBLAN system are solved numerically. The calculated population dynamics and output characteristics are derived and the ideas presented in Section II are investigated. The rate equations and parameters that are used for the calculation are presented here in detail for a better interpretation of the simulation and in order to make its predictions a more valuable tool for the experimentalist.

Recent progress in pump sources and active materials has generated the technical basis for an efficiently diode-pumped erbium 3-μm fiber laser. The following facts are exploited. First, cladding-pumped double-clad fiber systems allow for efficient diode pumping and high output-beam quality [13]. Double-clad ZBLAN fibers are now available, e.g., from Le Verre Fluoré. Special cladding geometries [14] or an acentric core allow for an effective absorption coefficient that is given by

$$\alpha_{\text{eff}} = (\omega_{\text{core}}/\omega_{\text{clad}})^2 \alpha \tag{1}$$

where α is the absorption coefficient at the pump wavelength and ω_{core}, ω_{clad} are the radii of core and inner cladding, respectively.

Second, two polarization-coupled diode lasers emitting at $\lambda_p = 795$ nm, capable of delivering $P_{\text{in}} = 7$-W power incident on the fiber, can be focused down to 25-μm radius with a N.A. of 0.2 [15] using a beam-shaping technique [16]. Coupling of these devices into a fiber with an inner cladding radius of $\omega_{\text{clad}} = 35$ μm and a $\text{N.A.}_{\text{clad}}$ of 0.25 has been experimentally demonstrated with an efficiency of 85%. Here a smaller coupling efficiency of $\eta_{\text{in}} = 75\%$ is assumed. A fraction of

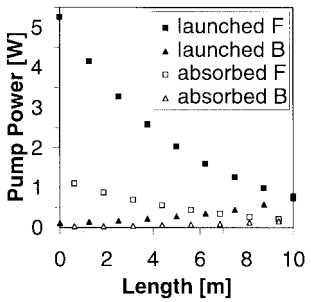

Fig. 2. Launched and absorbed pump power in forward direction (F) and after reflection by the mirror at the rear fiber end (B) versus fiber length.

$\eta_{\text{back}} = 95\%$ of the transmitted pump power is reflected back into the fiber by the rear mirror. Slightly different efficiencies may finally be obtained in an experimental approach, but this will not influence the general statements of this paper. Only the obtained output power will vary in a similar way as the coupling efficiencies.

The pump radiation is absorbed in the fiber core of radius $\omega_{\text{core}} = 4$ μm on the ground-state transition ${}^4I_{15/2} \rightarrow {}^4I_{9/2}$ as well as on the excited-state transitions [17] ${}^4I_{13/2} \rightarrow {}^2H_{11/2}$ and ${}^4I_{11/2} \rightarrow {}^4F_{5/2}$ (see Fig. 1). The absorption cross sections [4] of these transitions at 791 nm are $\sigma_{03} = 0.47 \times 10^{-21}$ cm^2, $\sigma_{15} = 1.0 \times 10^{-21}$ cm^2, and $\sigma_{27} = 0.2 \times 10^{-21}$ cm^2, respectively. From the measured spectrum of ESA from the ${}^4I_{13/2}$ level [18], it is apparent that detuning the pump to a wavelength is possible at which the ESA cross section is reduced to one third of its peak value or $\sigma_{15} = 0.33 \times 10^{-21}$ cm^2. This value is assumed in the calculation. An erbium concentration of 3.2×10^{20} cm^{-3} ($= 20\,000$ ppm mol. in ZBLAN) and a fiber length of $\ell = 10$ m ensure that more than 90% of the launched pump power are absorbed in the fiber (see Fig. 2).

The Er^{3+}:ZBLAN lifetimes τ_i which are given in Fig. 1 are partly taken from [12]. They represent the intrinsic lifetimes of the system at low dopant concentration and include radiative as well as multiphonon relaxations. The ${}^4S_{3/2}$ and ${}^2H_{11/2}$ levels are thermally coupled and are treated as a combined level in the same way as in [19]. The lifetime of the ${}^4F_{9/2}$ level is estimated from the corresponding lifetime in $LiYF_4$. The values of the ${}^4F_{7/2}$ and ${}^4F_{5/2}$ lifetimes are assumed. It was found in previous simulations that the values of these lifetimes are not crucial for the calculation [4], [19]. The branching ratios β_{ij} are calculated from Judd–Ofelt data of ZBLAN [12] with the procedure used in [19] under consideration of the fluorescence lifetimes of Fig. 1. They are found to be similar to those of $LiYF_4$ [19].

The lifetime quenching of the erbium ${}^4I_{11/2}$ and ${}^4I_{13/2}$ laser levels of the 2.7-μm transition by Pr^{3+} co-doping was experimentally investigated in ZBLAN [12], [20] and BaY_2F_8 [21]. In both cases, a strong quenching of the lifetime of the lower laser level versus a moderate quenching of the upper-level lifetime was found. The values [12], [20] obtained for 40 000 ppm mol. erbium concentration in ZBLAN are given in Table I. In this paper, it is assumed that a similar lifetime quenching can be obtained with an erbium concentration of 20 000 ppm mol. The required praseodymium concentrations

TABLE I
LIFETIME QUENCHING BY Pr^{3+} CO-DOPING OF THE $^4I_{11/2}$ AND $^4I_{13/2}$ LASER LEVELS OF THE 2.7-μm TRANSITION IN ERBIUM ZBLAN AS MEASURED IN [12] AND [20]

Pr^{3+} conc.	τ ($^4I_{11/2}$)	τ ($^4I_{13/2}$)
0 ppm	6.8 ms	8.7 ms
500 ppm	4 ms	1.6 ms
1000 ppm	3 ms	0.9 ms
2000 ppm	2.5 ms	0.3 ms
5000 ppm	1.5 ms	0.1 ms

The data are valid for an erbium concentration of 40000 ppm mol.

will probably be higher than those reported in [12] and [20] because of the smaller erbium concentration. The lifetimes used for the simulation correspond to a Pr^{3+} concentration of 2000 ppm mol.: $\tau_2 = 2.5$ ms, $\tau_1 = 0.3$ ms. Since these parameters are of utmost importance for the performance of the 2.7-μm laser as will be shown later, reliable data will have to be obtained from lifetime measurements in Pr^{3+} co-doped ZBLAN glass preforms prior to laser experiments. A clear and unquestionable tendency, however, is found in this paper even with the approximated data. Using higher erbium concentration in combination with detuning the pump wavelength from the GSA peak is a possible alternative to ensure sufficient lifetime quenching. It leads to results which are similar to those presented in the following sections.

As pointed out in Section II, two laser transitions are relevant for the system: from $^4I_{11/2} \rightarrow {}^4I_{13/2}$ at $\lambda_{21} = 2.7$ μm and from $^4S_{3/2} \rightarrow {}^4I_{13/2}$ at $\lambda_{51} = 850$ nm (see Fig. 1). The actual Stark transition of the 2.7-μm laser is not of large relevance here, because it only influences the threshold which is calculated to be in the range of 1 mW. Thermal redistribution within each multiplet is assumed to take place instantaneously. For consistency with [4], [7], and [9], let the 2.7-μm laser originate from the second Stark level of the $^4I_{11/2}$ multiplet. The 850-nm laser is assumed to originate from the first Stark level of the $^4S_{3/2}$ multiplet. Both laser transitions shall terminate in the fourth Stark level of the $^4I_{13/2}$ multiplet. Since the Stark-level energies of erbium are inhomogeneously broadened in ZBLAN and cannot be measured, the Boltzmann factors of upper and lower Stark laser levels are taken from $LiYF_4$ [4], [7]. Values at 300 K are $b_2 = 0.200$, $b_1 = 0.113$, and $b_5 = 0.533$. The degeneracies are $g_1 = g_2 = g_5 = 2$.

The radiatively emitted fractions of the rates from upper to lower laser levels are $\gamma_{21} = 0.4$ at 2.7 μm [7] and $\gamma_{51} = 1$ at 850 nm. The geometrical and spectral fractions of the emitted fluorescence which are coupled into the fiber mode are assumed as $P_\theta = 10^{-2}$ [4] and $P_\nu = 10^{-4}$, respectively. These values influence the behavior of the relaxation oscillations but are not of relevance for the present investigation. The stimulated-emission cross sections are $\sigma_{21} = 0.57 \times 10^{-21}$ cm^2 at 2.7 μm [12] and $\sigma_{51} = 0.6 \times 10^{-21}$ cm^2 at 850 nm [9]. The reflectances of incoupling (1) and outcoupling (2) mirrors are assumed as $Rf1_{21} = 99.8\%$, $Rf2_{21} = 85\%$ at 2.7 μm and $Rf1_{51} = Rf2_{51} = 15\%$ at 850 nm. The losses in ZBLAN fiber are assumed as follows: $\kappa_{21} = 1$ dB/km ($= 0.23$ km^{-1}) at 2.7 μm and $\kappa_{51} = 2$ dB/km ($= 0.46$ km^{-1}) at 850 nm. In newly fabricated ZBLAN fibers, measured values of the losses at these wavelengths are approximately an order of magnitude smaller [12], but degradation in fiber quality is taken into account here by the assumption of higher losses. The optical fiber length is $\ell_{\rm opt} = 15$ m. With a N.A.$_{\rm core}$ of, e.g., 0.25, transversely single-mode laser emission at 2.7 μm is obtained.

The possible influence of the three interionic processes referred to as W_{11}, W_{22}, and W_{50} in Fig. 1 is investigated in the simulation. The lifetime quenching of the $^4S_{3/2}/^2H_{11/2}$ multiplets via the cross-relaxation process W_{50} is strong [12], whereas the upconversion processes W_{11} and W_{22} seem to have a rather small influence in ZBLAN even at high erbium concentrations [12]. Since the parameters of the interionic upconversion processes W_{11} and W_{22} are only known for erbium concentrations of more than 1×10^{21} cm^{-3} ($=$ 60 000 ppm mol. in ZBLAN) in $LiYF_4$ [22] and BaY_2F_8 [21], the influence of these processes is investigated in the simulation for a large range of parameters. The parameter of the cross relaxation W_{50} is assumed to be in the same order of magnitude. The inverse interionic processes are not taken into account here.

h and c denote Planck's constant and the vacuum speed of light, respectively. For the simulation, cylindrical and radially homogeneous profiles of pump and laser mode are assumed. Let z be the variable of the length. It may be a continuous variable extending from 0 to ℓ or, in this case, represent the discrete longitudinal elements 1 to n covering the fiber length ℓ. With the above considerations, the rate equations for the population densities $N_i(z)$ read

$$dN_7(z)/dt = R_{27}(z) - \tau_7^{-1} N_7(z) \tag{2}$$

$$dN_6(z)/dt = -\tau_6^{-1} N_6(z) + \beta_{76}\tau_7^{-1} N_7(z) + W_{22} N_2^2(z) \tag{3}$$

$$dN_5(z)/dt = R_{15}(z) - \tau_5^{-1} N_5(z) + \Sigma_{i=6..7}\left(\beta_{i5}\tau_i^{-1} N_i(z)\right) - W_{50} N_5(z) N_0(z) - \mathrm{SE}_{51}(z) \tag{4}$$

$$dN_4(z)/dt = -\tau_4^{-1} N_4(z) + \Sigma_{i=5..7}\left(\beta_{i4}\tau_i^{-1} N_i(z)\right) \tag{5}$$

$$dN_3(z)/dt = R_{03}(z) - \tau_3^{-1} N_3(z) + \Sigma_{i=4..7}\left(\beta_{i3}\tau_i^{-1} N_i(z)\right) + W_{50} N_5(z) N_0(z) + W_{11} N_1^2(z) \tag{6}$$

$$dN_2(z)/dt = -R_{27}(z) - \tau_2^{-1} N_2(z) + \Sigma_{i=3..7}\left(\beta_{i2}\tau_i^{-1} N_i(z)\right) - 2W_{22} N_2^2(z) - \mathrm{SE}_{21}(z) \tag{7}$$

$$dN_1(z)/dt = -R_{15}(z) - \tau_1^{-1} N_1(z) + \Sigma_{i=2..7}\left(\beta_{i1}\tau_i^{-1} N_i(z)\right) + W_{50} N_5(z) N_0(z) - 2W_{11} N_1^2(z) + \mathrm{SE}_{21}(z) + \mathrm{SE}_{51}(z) \tag{8}$$

$$dN_0(z)/dt = -R_{03}(z) + \Sigma_{i=1..7}\left(\beta_{i0}\tau_i^{-1} N_i(z)\right) - W_{50} N_5(z) N_0(z) + W_{11} N_1^2(z) + W_{22} N_2^2(z). \tag{9}$$

The absorption coefficient $\alpha(z)$ within the longitudinal spatial element z of width $\Delta\ell(z)$ and the launched powers $P_l'(z)$ and $P_l''(z)$ of front-mirror-coupled and end-mirror-reflected pump

radiation, respectively, are given by

$$\alpha(z) = \sigma_{03}N_0(z) + \sigma_{15}N_1(z) + \sigma_{27}N_2(z) \tag{10}$$

$$P_l'(z) = \eta_{\text{in}}P_{\text{in}} \prod_{z'=1}^{z-1} \{\exp[-\Delta\ell(z')\alpha(z')(\omega_{\text{core}}/\omega_{\text{clad}})^2]\} \tag{11}$$

$$P_l''(z) = P_l'(n)\exp[-\Delta\ell(n)\alpha(n)(\omega_{\text{core}}/\omega_{\text{clad}})^2] \times \eta_{\text{back}} \prod_{z'=n}^{z+1} \{\exp[-\Delta\ell(z')\alpha(z')(\omega_{\text{core}}/\omega_{\text{clad}})^2]\}. \tag{12}$$

With (10)–(12), the equation for the pump rate $R_{ij}(z)$ on the transition from level i into level j reads

$$R_{ij}(z) = (\sigma_{ij}N_i(z)/\alpha(z))\{1 - \exp[-\Delta\ell(z)\alpha(z) \times (\omega_{\text{core}}/\omega_{\text{clad}})^2]\}\lambda_p/(hc\ell\pi\omega_{\text{core}}^2)(P_l'(z) + P_l''(z)) \tag{13}$$

Equation (13) considers ground-state depletion and population of an ESA level dynamically. The rate equation for the photon density ϕ_{ij} on the transition from level i into level j is given by

$$d\phi_{ij}/dt = (\ell/\ell_{\text{opt}}) \sum_{z=1}^{n} [P_\theta P_\nu \gamma\beta_{ij}\tau_i^{-1}N_i(z) + \text{SE}_{ij}(z)] - [-\ln(Rf1_{ij}Rf2_{ij}) + 2\kappa_{ij}\ell]c\phi_{ij}/(2\ell_{\text{opt}}). \tag{14}$$

The stimulated-emission rate $\text{SE}_{ij}(z)$ on the transition from level i into level j is

$$\text{SE}_{ij}(z) = [b_iN_i(z) - (g_i/g_j)b_jN_j(z)]\sigma_{ij}c\phi_{ij}. \tag{15}$$

The output power $P_{\text{out},ij}$ on the transition from level i into level j is calculated from the equation

$$P_{\text{out},ij} = c\phi_{ij}(hc/\lambda_{ij})\pi\omega_{\text{core}}^2(1 - Rf2_{ij}). \tag{16}$$

The rate equations are solved with a longitudinal resolution of the active medium of $n = 8$ elements of equal length and in a Runge–Kutta calculation of fourth order. The relaxation oscillations which occur when the laser reaches threshold are suppressed in the time-resolved investigation in order to obtain nonoscillating values for the pump-pulse dependent slope efficiency also in the region of the oscillations. For all calculations, Er^{3+} and Pr^{3+} concentrations of 20 000 ppm mol. and 2000 ppm mol., respectively, and an incident pump power of 7 W (with the exception of Fig. 5, where the incident power is varied) are assumed. Results are given in Figs. 2–9.

IV. Performance Under CW and Pulsed Excitation

In this section, the calculated pump distribution, CW laser operation, excitation density, and the GSA and ESA pump rates of the system are presented and discussed. In addition, the behavior under pulsed excitation for the generation of laser pulses is investigated.

Fig. 2 shows the fractions of launched and absorbed pump power in forward direction and after reflection by the mirror

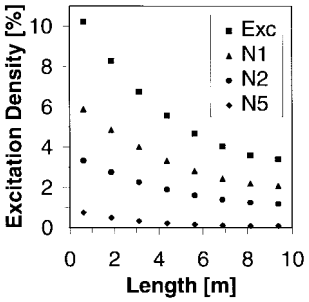

Fig. 3. Excitation density (Exc) and the population densities of the important levels ${}^4I_{13/2}$ (N_1), ${}^4I_{11/2}$ (N_2), and ${}^4S_{3/2} + {}^2H_{11/2}$ (N_5) in percent of the dopant concentration versus fiber length.

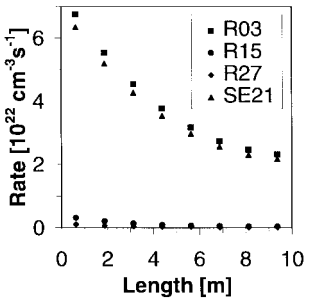

Fig. 4. Calculated pump rates R_{03} (GSA from ${}^4I_{15/2}$), R_{15} (ESA 1 from ${}^4I_{13/2}$), R_{27} (ESA 2 from ${}^4I_{11/2}$), and stimulated emission SE_{21} at 2.7 μm versus fiber length.

at the rear fiber end. The chosen combination of dopant concentration, absorption coefficient, cladding and core radii, fiber length, high reflection from the rear mirror, Pr^{3+} co-doping, and Er^{3+} lifetimes leads to an efficient pump absorption of 97% (1% and 2% loss at the rear and front fiber ends, respectively). A relatively uniform distribution of the absorbed pump power is obtained. This is important in order to avoid a strong influence of ESA in the first part of the fiber.

High dopant concentration, low pump density, low effective absorption coefficient, and strong lifetime quenching lead to an excitation density (Fig. 3) which is comparatively low. Consequently, the rates of ESA from the laser levels are very small (Fig. 4), and most of the pump rate is converted into stimulated emission (Fig. 4). The small ESA rate also implies that the excitation of the ${}^4S_{3/2}$ level remains small (Fig. 3). The 850-nm laser does not reach threshold and an uncontrolled redistribution of the excitation of the ${}^4S_{3/2}$ level is avoided. Thus the combined goal of reduced ground-state bleaching and reduced ESA is satisfactorily fulfilled.

The corresponding input–output curve is shown in Fig. 5 (squares). A transversely single-mode output power of 1.02 W is predicted by the simulation. The output intensity in the range of 1.8 MW/cm^2 is of high relevance for surgical applications. The behavior indicates that the saturation of the output power is almost completely absent in this low-pump-intensity approach. The calculated slope efficiency (solid line) is 15% versus incident pump power and 19% versus launched pump power. The latter value represents two third of the Stokes efficiency of 29%, which is a reasonable fraction for a four-level laser. The missing part is sacrificed for the long fiber

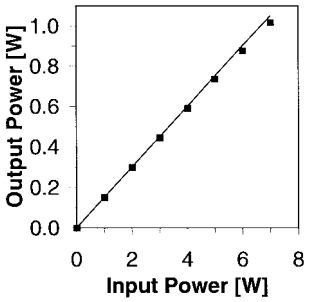

Fig. 5. Calculated input–output curve (squares) of the double-clad diode-pumped erbium 2.7-μm fiber laser. The slope efficiency (solid line) is 15% versus incident pump power and 19% versus launched pump power. The threshold is in the order of a few milliwatts. The small saturation effect of the output power at high pump power is owing to the onset of ESA losses.

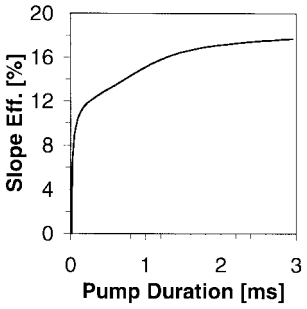

Fig. 6. Temporal evolution of the slope efficiency with respect to launched pump energy under pulsed excitation. Relaxation oscillations are suppressed in this simulation.

length and efficient pump absorption, because the loss per unit length at 2.7 μm is assumed rather high in this calculation. A smaller loss and a higher slope efficiency and output power will probably be obtained experimentally with a new ZBLAN fiber. A small deviation from the slope efficiency at low pump power (solid line) is visible at high pump power. This indicates the onset of the influence of ESA losses. This slight saturation of the output power will increase at higher pump power. It can be avoided by using a larger cladding radius (or smaller GSA coefficient) in combination with a longer fiber.

The present approach has further practical advantages. A damage of the coating of the input mirror is avoided due to the low pump intensity. If the laser is operated in a cascade regime, the wavelength specifications of the mirror coatings are stringent [5], [6], [23]. It was not possible in these situations to optimize the mirror reflectance at 2.7 μm, because the requirements at 1.7 μm and 850 nm had to be fulfilled. In the present approach, the requirement at 1.7 μm can be omitted and the requirement at 850 nm is less strict. This allows for the manufacture of mirrors that have high reflectance at 2.7 μm and high transmission at 800 nm (input mirror) or medium transmission at 2.7 μm and high reflectance at 800 nm (output mirror). The cavity alignment is also less critical, because the high-gain 850-nm line does not have to be suppressed by the low-gain 1.7-μm laser [5], [23].

Surgery with 3-μm laser radiation brought to the operation site via endoscope as, e.g., in orthopedy, is normally performed in aqueous media. Long pulses (pulse duration 400 μs) lead to an optimum in efficiency of tissue ablation [3] when applied in liquid surroundings. Laser pulses of this duration can be generated by pulsed excitation of the laser. However, pulsed excitation of an erbium 3-μm laser affects the efficiency of the laser output. A strong decrease in efficiency with shortening of the pump-pulse duration was found in erbium-doped crystal lasers [24]–[26] which are operated in an interionic-upconversion regime. These lasers reach their high slope efficiency of up to 50% under Ti:sapphire pumping [27] or 35% under diode-pumping [28] only after the establishment of a high excitation density which supports the upconversion process. At a pump-pulse duration of 400 μs, their slope efficiency is less than 20% [25], [26]. Nevertheless, a high efficiency of the laser output is essential for clinical applications.

Since the fiber laser can be operated in a simple four-level regime with low excitation density, it reaches its CW slope efficiency much faster. As can be seen from Fig. 6, the slope efficiency is already 70% of its CW value after a pump duration of 400 μs. In this calculation, the slope efficiency is slightly higher than that in Fig. 5, because the relaxation oscillations at the onset of laser emission are suppressed by assuming a higher fraction of the spontaneous emission at 2.7 μm coupled into the laser mode. The same procedure was applied in [25] for the calculation of the slope efficiency of the crystal laser. The result of Fig. 6 shows that the smaller slope efficiency of the 3-μm fiber laser compared to the 3-μm crystal laser is partly compensated in the pulsed regime.

V. Possible Drawbacks

The influence of insufficient absorption in double-clad fibers and competitive lasing at 850 nm is abolished by the measures explained in the previous sections. Several other processes such as ESA losses at certain pump wavelengths, high dopant concentration and the introduction of losses due to interionic processes, as well as insufficient lifetime quenching may, however, affect the laser performance at 2.7 μm in a negative way. The behavior of the 2.7-μm fiber-laser system under these circumstances is subject to a quantitative investigation in this section.

Let us first consider the influence of ESA from the lower or upper laser level when tuning the pump wavelength. Within the 800-nm GSA band of erbium, there are two ESA transitions (cf. Fig. 1): ESA 1 originates from the lower laser level [18] and has an absorption peak at 791 nm. ESA 2 from the upper laser level [17] has a maximum at longer wavelengths around 810 nm [29]. As is expected from the discussion in Section II, the increase of ESA 1 from the lower laser level has a negative influence (cf. Fig. 7), because the ground state is now sufficiently populated to guarantee pump absorption, which undermines the previously positive influence of this ESA, and the energy upconverted by ESA 1 is only partly redistributed into the upper laser level and, therefore, only partly converted into laser emission at 2.7 μm. The second ESA from the upper laser level has an even more detrimental influence on lasing, because it removes population from the upper laser level without any contribution to lasing at 2.7 μm.

However, a very positive result of the efforts which were made in the previous Sections to reduce the excitation density

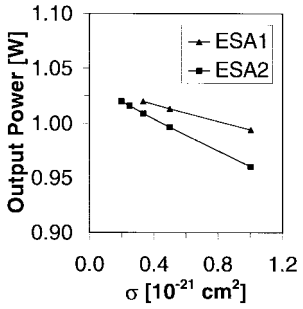

Fig. 7. The influence of ESA 1 from the ${}^4I_{13/2}$ lower laser level and ESA 2 from the ${}^4I_{11/2}$ upper laser level on the calculated output power. The lowest values of each ESA cross section are the initial values used for all calculations.

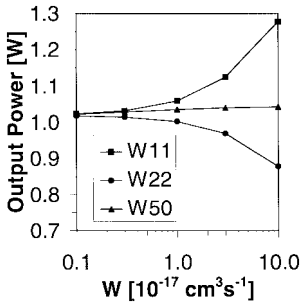

Fig. 8. The influence of upconversion W_{11} from the ${}^4I_{13/2}$ lower laser level, upconversion W_{22} from the ${}^4I_{11/2}$ upper laser level, and cross relaxation from the ${}^4S_{3/2} + {}^2H_{11/2}$ levels on the calculated output power.

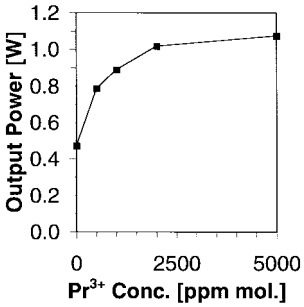

Fig. 9. The influence of lifetime quenching by Pr^{3+} co-doping on the calculated output power. The values of the lifetimes of upper and lower laser levels for different Pr^{3+} concentrations are taken from [12] and [20] and are reproduced in Table I. The given Pr^{3+} concentrations and Er^{3+} lifetimes are valid for 40000 ppm mol. Er^{3+} concentration, whereas the Er^{3+} concentration used for the calculation is 20 000 ppm mol.

of the system is highlighted by Fig. 7 as well: The influence of ESA losses on the output power is small (less than 10%) even for extremely high ESA cross sections. That is, the pump wavelength can be tuned back to the peak of ESA from the lower laser level at 791 nm without significantly decreasing the performance of the 2.7-μm laser. In practice, this means that the pump wavelength can be chosen to best match the GSA cross section for efficient and well-distributed pump absorption without severe restrictions introduced by ESA. In addition, diode lasers can be used for pumping without a temperature stabilization of the pump wavelength. This is a major advantage. It may be even possible to pump the system in the 980-nm band directly into the ${}^4I_{11/2}$ upper laser level, which enhances the Stokes efficiency of the system from 29% to 35%, despite the fact that there is a strong ESA in erbium at this pump wavelength originating from the upper laser level [30], [31].

The chosen dopant concentration is in principle high enough to introduce a strong influence of interionic processes (cf. Fig. 1) on the population dynamics of the system. It can be concluded from concentration-dependent lifetime measurements [12] that the quenching of the ${}^4S_{3/2}$ lifetime by the cross relaxation W_{50} is indeed significant. On the other hand, no measurable reduction of the lifetimes of the laser levels by the upconversion processes W_{11} and W_{22} up to an erbium concentration of 40 000 ppm mol. was found in the same experiment, indicating that the corresponding parameters are small.

Fig. 8 displays the influence of the three interionic processes on the laser output power for a large range of parameters. The sign of the influence is the same as was found for 3-μm crystal lasers [19]. The energy recycling by upconversion W_{11} or cross relaxation W_{50} is beneficial for lasing, whereas the depletion of the upper laser level by upconversion W_{22} is detrimental to lasing. The magnitude of the influence of all three processes, however, is much smaller than in the crystal laser. This is again a result of the small excitation density predicted in Section IV.

Although the lifetime of the ${}^4S_{3/2}$ and ${}^2H_{11/2}$ levels is quenched in the simulation from 520 to 50 μs by increasing the parameter of the cross-relaxation W_{50}, its influence is marginal, because the ESA and upconversion rates that lead to the excitation of the ${}^4S_{3/2}$ and ${}^2H_{11/2}$ levels are small. The cross relaxation saturates as soon as it seizes the whole population of these levels (cf. Fig. 8). The influence of the upconversion processes on output power increases to some 20%, if extremely high parameters are assumed. Even if such high parameters were present in ZBLAN glass, the parameters W_{11} and W_{22} would probably be in the same order of magnitude (cf. [21], [22]) and the upconversion processes would merely compensate each other.

An interesting difference between the ESA and upconversion losses shall be pointed out here. As can be derived from (10) and (13), the ESA losses depend on both the absolute and the relative population density of the initial levels. The upconversion rates, on the other hand, depend only on the absolute population densities of the initial levels [cf., e.g., (9)] and are, therefore, less well suppressed by the measures taken in the previous sections.

The crucial parameter of the whole investigation is found to be the value of the lifetime quenching of the lower laser level by Pr^{3+} co-doping. The lifetimes of the laser levels measured [12], [20] for several Pr^{3+} concentrations at 40000 ppm mol. Er^{3+} concentration are given in Table I. The lifetime quenching of the upper laser level by Pr^{3+} co-doping is smaller than the quenching of the lower-level lifetime, and CW inversion is maintained. The detrimental result of insufficient lifetime quenching can be examined in Fig. 9. The excitation density is strongly increased by insufficient quenching, ground-state bleaching reoccurs, ESA losses gain a large influence, and the output power at 2.7 μm drops significantly. It has, therefore, to be checked spectroscopically whether and at which Pr^{3+}

concentration a sufficient lifetime quenching can be achieved with 20 000 ppm mol. Er^{3+} concentration.

The positive result of the improvements of the previous sections is also visible in Fig. 9. Even in the worst case without any lifetime quenching the calculation predicts that the diode-pumped laser will emit an output power of almost 500 mW, which is by far more than has been demonstrated in the highly efficient Ti:sapphire-pumped cascade regimes [5], [6].

VI. Conclusion

A new approach toward a diode-pumped erbium 3-μm fiber laser was investigated in computer simulations. ESA was identified as the major problem of this laser. It could be shown that the combination of lifetime quenching by Pr^{3+} co-doping, a high erbium concentration, and pumping with low pump intensity at wavelengths with small ESA cross sections will lead to sufficient pump absorption, a small excitation density, and a simple four-level system without a significant influence of ESA.

With the assumption of state-of-the-art technology including double-clad diode pumping, an output power of 1.0 W and a slope efficiency of 15% versus incident pump power and 19% versus launched pump power are predicted. The corresponding output intensity in the range of 1.8 MW/cm^2 is of high relevance for surgical applications. At a pump-pulse duration of 400 μs, which leads to efficient ablation of biotissue in liquid surroundings, the ZBLAN laser can reach 70% of its CW power. Compared to Ti:sapphire-pumped cascade-lasing regimes in ZBLAN, the proposed approach represents a strong decrease of the requirements on mirror coatings, cavity alignment, and especially pump intensity. Possible drawbacks of this approach such as increased ESA by detuning the pump wavelength or interionic processes are found to be of minor influence as long as a sufficient lifetime quenching of the lower laser level is ensured. Even without lifetime quenching the proposed diode-pumped laser is capable of emitting almost 500 mW at 2.7 μm, which will represent a strong improvement compared to present devices, which operate at only 150 mW output power and are restricted to Ti:sapphire pumping.

Acknowledgment

The author thanks W. Lüthy and H. P. Weber from the Institute of Applied Physics, University of Bern, Switzerland, for helpful discussions.

References

[1] L. Esterowitz and R. Allen, "Rare earth doped IR fiber lasers for medical applications," *SPIE Infrared Fiber Optics*, vol. 1048, pp. 129–132, 1989.

[2] S. L. Jacques and G. Gofstein, *SPIE Laser-Tissue Interaction II*, vol. 1427, p. 63, 1991.

[3] M. Ith, H. Pratisto, H. J. Altermatt, M. Frenz, and H. P. Weber, "Dynamics of laser-induced channel formation in water and influence of pulse duration on the ablation of biotissue under water with pulsed erbium-laser radiation," *Appl. Phys. B*, vol. 59, no. 6, pp. 621–629, 1994.

[4] S. Bedö, M. Pollnau, W. Lüthy, and H. P. Weber, "Saturation of the 2.71 μm laser output in erbium doped ZBLAN fibers," *Opt. Commun.*, vol. 116, nos. 1–3, pp. 81–86, 1995.

[5] M. Pollnau, Ch. Ghisler, G. Bunea, M. Bunea, W. Lüthy, and H. P. Weber, "150 mW unsaturated output power at 3 μm from a single-mode-fiber erbium cascade laser," *Appl. Phys. Lett.*, vol. 66, no. 26, pp. 3564–3566, 1995.

[6] M. Pollnau, Ch. Ghisler, W. Lüthy, H. P. Weber, J. Schneider, and U. B. Unrau, "Three-transition cascade erbium laser at 1.7, 2.7, and 1.6 μm," *Opt. Lett.*, vol. 22, no. 9, pp. 612–614, 1997.

[7] M. Pollnau, R. Spring, Ch. Ghisler, S. Wittwer, W. Lüthy, and H. P. Weber, "Efficiency of erbium 3-μm crystal and fiber lasers," *IEEE J. Quantum Electron.*, vol. 32, pp. 657–663, Apr. 1996.

[8] J. Schneider, D. Hauschild, C. Frerichs, and L. Wetenkamp, "Highly efficient Er^{3+}:Pr^{3+}-codoped cw fluorozirconate fiber laser operating at 2.7 μm," *Int. J. Infrared Millimeter Waves*, vol. 15, pp. 1907–1922, 1994.

[9] M. Pollnau, J. Schneider, U. B. Unrau, W. Lüthy, and H. P. Weber, "Pr^{3+} co-doped 2.8-μm erbium fiber laser," in *Conf. Lasers and Electro-Optics/Europe 1996, Tech. Dig.*, p. 132, paper CTuL6.

[10] R. S. Quimby and W. J. Miniscalco, "Continuous-wave lasing on a self-terminating transition," *Appl. Opt.*, vol. 28, no. 1, pp. 14–16, 1989.

[11] S. Bedö, W. Lüthy, and H. P. Weber, "Limits of the output power in Er^{3+}: ZBLAN single-mode fiber lasers," *Electron. Lett.*, vol. 31, no. 3, pp. 199–200, 1995.

[12] L. Wetenkamp, "Charakterisierung von laseraktiv dotierten Schwermetallfluorid-Gläsern und Faserlasern," Ph.D. dissertation, Institute of High-Frequency Technique, Technical Univ. of Braunschweig, Germany, 1991.

[13] H. Zellmer, U. Willamowski, A. Tünnermann, H. Welling, S. Unger, V. Reichel, H. R. Müller, J. Kirchhof, and P. Albers, "High-power cw neodymium-doped fiber laser operating at 9.2 W with high beam quality," *Opt. Lett.*, vol. 20, no. 6, pp. 578–580, 1995.

[14] M. H. Muendel, "Optimal inner cladding shapes for double-clad fiber lasers," in *Conf. Lasers and Electro-Optics, 1996 OSA Tech. Dig. Ser.*, Washington, DC, vol. 9, p. 209, paper CTuU2.

[15] G. J. Friel, W. A. Clarkson, and D. C. Hanna, "High-gain Nd:YLF amplifier end-pumped by a beam-shaped broad-stripe diode laser," in *Conf. Lasers and Electro-Optics, 1996 OSA Tech. Dig. Ser.*, Washington, DC, vol. 9, p. 144, paper CTuL28.

[16] W. A. Clarkson and D. C. Hanna, "Two-mirror beam-shaping technique for high-power diode bars," *Opt. Lett.*, vol. 21, no. 6, pp. 375–377, 1996.

[17] M. Pollnau, E. Heumann, and G. Huber, "Time-resolved spectra of excited-state absorption in Er^{3+} doped $YAlO_3$," *Appl. Phys. A*, vol. 54, no. 5, pp. 404–410, 1992.

[18] L. Esterowitz, R. Allen, and I. Aggarwal, "The effects of excited-state absorption on the cw operation of the erbium $^4I_{11/2} \rightarrow {}^4I_{13/2}$ fiber laser," in *Advanced Solid-State Lasers, 1991 Tech. Dig. Ser.*, Washington, DC, pp. 160–162.

[19] M. Pollnau, Th. Graf, J. E. Balmer, W. Lüthy, and H. P. Weber, "Explanation of the cw operation of the Er^{3+} 3-μm crystal laser," *Phys. Rev. A*, vol. 49, no. 5, pp. 3990–3996, 1994.

[20] L. Wetenkamp, G. F. West, and H. Többen, "Co-doping effects in erbium^{3+}- and holmium^{3+}-doped ZBLAN glass," *J. Non-Crystalline Sol.*, vol. 140, pp. 25–30, 1992.

[21] D. S. Knowles and H. P. Jenssen, "Upconversion versus Pr-deactivation for efficient 3 μm laser operation in Er," *IEEE J. Quantum Electron.*, vol. 28, pp. 1197–1208, Apr. 1992.

[22] H. Chou and H. P. Jenssen, "Upconversion processes in Er-activated solid state laser materials," in *Tunable Solid State Lasers, of the OSA Proceeding Series*, M. L. Shand and H. P. Jenssen, Eds. Washington DC: Opt. Soc. Amer., 1989, vol. 5, pp. 167–174.

[23] Ch. Ghisler, M. Pollnau, G. Bunea, M. Bunea, W. Lüthy, and H. P. Weber, "Up-conversion cascade laser at 1.7 μm with simultaneous 2.7 μm lasing in erbium ZBLAN fiber," *Electron. Lett.*, vol. 31, no. 5, pp. 373–374, 1995.

[24] A. M. Prokhorov, V. I. Zhekov, T. M. Murina, and N. N. Platnov, "Pulsed YAG:Er^{3+} laser efficiency (analysis of model equations)," *Laser Phys.*, vol. 3, pp. 79–83, 1993.

[25] M. Pollnau, R. Spring, S. Wittwer, W. Lüthy, and H. P. Weber, "Investigations on the slope efficiency of a pulsed 2.8-μm Er^{3+}:$LiYF_4$ laser," *J. Opt. Soc. Amer. B*, vol. 14, no. 4, pp. 974–978, 1997.

[26] T. Jensen, G. Huber, and K. Petermann, "Quasi-cw diode pumped 2.8 μm laser operation of Er^{3+}-doped garnets," in *Advanced Solid-State Lasers, Tech. Dig.*, Washington, DC, 1996, pp. 265–267.

[27] Ch. Wyss, W. Lüthy, H. P. Weber, P. Rogin, and J. Hulliger, "Emission properties of an optimized 2.8 μm Er^{3+}:YLF laser," *Opt. Commun.*, vol. 139, pp. 215–218, 1997.

[28] T. Jensen, A. Diening, G. Huber, and B. H. T. Chai, "Investigation of diode-pumped 2.8-μm Er:$LiYF_4$ lasers with various doping levels," *Opt. Lett.*, vol. 21, no. 8, pp. 585–587, 1996.

[29] S. Zemon, G. Lambert, W. J. Miniscalco, R. W. Davies, B. T. Hall, R. C. Folweiler, T. Wei, L. J. Andrews, and M. P. Singh, "Excited state cross sections for Er-doped glasses," *SPIE Fiber Laser Sources and Amplifiers II*, vol. 1373, pp. 21–32, 1990.
[30] R. S. Quimby, W. J. Miniscalco, and B. Thompson, "Excited state absorption at 980 nm in erbium doped glass," *SPIE Fiber Laser Sources and Amplifiers III*, vol. 1581, pp. 72–79, 1991.
[31] M. Pollnau, W. Lüthy, H. P. Weber, K. Krämer, H. U. Güdel, and R. A. McFarlane, "Excited-state absorption in Er:BaY_2F_8 and $Cs_3Er_2Br_9$ and comparison with Er:$LiYF_4$," *Appl. Phys. B*, vol. 62, no. 4, pp. 339–344, 1996.

Markus Pollnau received the Diploma in physics from the University of Hamburg, Germany, in 1992 and the Ph.D. degree in physics from the University of Bern, Switzerland, in 1996.

Currently, he is with the Optoelectronics Research Centre at the University of Southampton, Southampton, U.K., as a Post-Doctoral Research Fellow of the European Union. His scientific work on solid-state lasers has included time-resolved spectroscopy, upconversion and cascade lasers, rate-equation analysis of population dynamics, thermal and thermooptical issues, Q-switching, and nonlinear frequency conversion.